Transactions of the Materials Research Society of Japan 29 [3] 1005-1010 (2004)

Ribbon-Formed Organosulfur Supramolecules for Novel Nanoenergy Devices

Katsuhiko Naoi* and Nobuhiro Ogihara
Graduate School of Technology,
Tokyo University of Agriculture & Technology,
2-24-16 Naka-cho, Koganei, Tokyo 184-8588, Japan
Fax: 81-42-387-8448, e-mail: k-naoi@cc.tuat.ac.jp

A novel ribbon-formed supramolecule interconnected via hydrogen bonds has been synthesized as sulfur-based energy storage materials utilized in supercapacitors and proton batteries. A nano-ordered composite was made with 2-amino-4,6-dimercaptopyrimidine (ADMP) suprmolecule adsorbed on graphite basal surfaces of nanocarbon namely Ketjen black (KB:diameter < 50 nm). From the results of cyclic voltammetric analysis, a ADMP/KB nanocomposite electrode has shown a reversible redox behavior for repeated cycles in 4 M H_2SO_4 and delivered a specific capacity of 247 mAh g^{-1} at a scan rate of 5 mV s^{-1} with high charge utilization (74 %). Moreover, the ADMP/KB electrode maintained 165 mAh g^{-1} at a high scan rate of 1000 mV s^{-1}. Such a high rate efficiency is considered to be attained by facile and reversible formation/reorganization of ribbon-formed supramolecular structure during redox proecess of ADMP.

Key words: 2-amino-4,6-dimercaptopyrimidine, disulfide bond, supramolecule, hydrogen bond, supercapacitor

1. INTRODUCTION

The authors attempted to design and synthesize a novel organosulfur compound, 2-amino-4,6-dimercaptopyrimidine (ADMP). In acidic aqueous media, the ADMPs organize self-complementary to form a continuous supramolecular ribbon with the aid of hydrogen bond (Scheme 1).

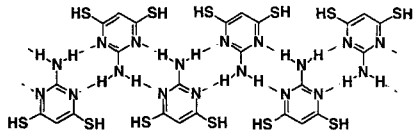

Scheme 1

As Lehn reported [1-8], such a nucleotide-like amino-pyrimidine structure is constructed where an amino group functions as proton donor and a pyrimidine ring as proton acceptor (Scheme 2).

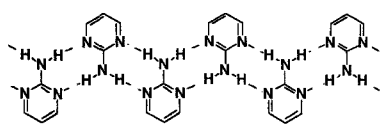

Scheme 2

The ADMP also has a free S-H group that serves as energy storage. The S-H group shows a reversible redox process accompanying a formation/cleavage of disulfide bond (S-S) (Figure 1) [9-21].

During the redox process of ADMPs, different oxidized/reduced states are formed. Formation and reorganization of supramolecular ADMP assembly occur more facile via relatively weak hydrogen bonds bcause the energy of hydrogen bond (4-120 kJ mol^{-1} [22]) is lower than that of the disulfide bond (120-260 kJ mol^{-1} [23]). The weak interaction of the ADMP assembly does not

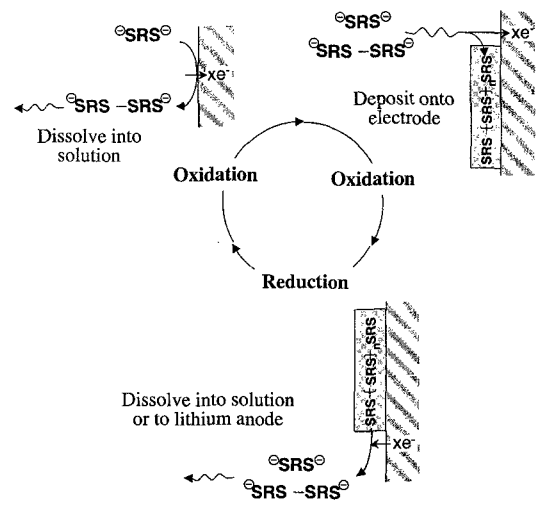

Fig.1 Schematic illustrations for the redox (polymerization-depolymerization accompanying a reversible chemical formation / cleavage of disulfide bonds) process of organosulfur compounds.

inhibit a reversible redox process of S-H/S-S. The ADMPs are always maintained self-associated to form different structures of supramolecular ribbons at every oxidized states in solutions.

For application to supercapacitors and proton batteries, we made a nanocomposite composed of ribbon-formed ADMP supramoelcules adsorbed on graphite surfaces of nano-meter ordered particles of Ketjen black (KB) as conducting agents. We examine the ADMP/KB nanocomposite electrode for their spectroscopic and electrochemical characteristics.

2. EXPERIMENTAL

2.1 Materials

A reagent grade of 2-amino-4,6-dichloropyrimidine and NaSH-nH_2O (Wako Chemilas) were used as received. A high grade of dimethylformamide (DMF), dimethylsulfoxide (DMSO), DMSO-d_6, and N-methylpyrrolidone (NMP) from Wako Chemicals were used as solvents. Ketjen black (KB: EC-600JD) were used as conducting agent. Carbon paper (TGP-H-030, Toray Ind.) was used as current collector. All the aqueous solutions were prepared with doubly distilled water.

2.2 Synthesis and characterization of 2-amino-4,6-dimercaptopyrimidine

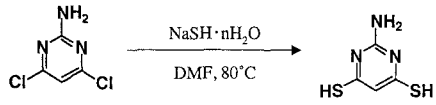

Scheme 3

NaSH-nH_2O (8.40 g, 150 mmol) was dissolved in dry DMF (60 ml) under argon atmosphere. 2-amino-4,6-dichloropyrimidine (4.92 g, 30 mmol) in dry DMF (90 ml) was added to the solution dropwise and was kept at 50 °C. The solution was stirred for 1 hour at 50 °C and was continued to be stirred for overnight at room temperature. The product was evaporated *in vacuo*, poured into water, and recrystallized from cold water (pH=2).

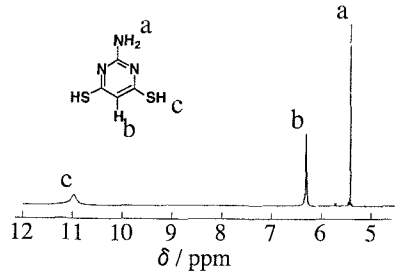

Fig.2 ^{1}H NMR of ADMP of DMSO-d_6 solution.

Finally, the ADMP was obtained with a 50 % yield as a light yellow needle crystal. Figure 2 shows the ^{1}H NMR spectrum for the ADMP in DMSO-d_6. The signals of 6.3 and 5.4 ppm are clearly identified as the phenyl ring and amino protons, respectively. The thiol proton was confirmed as a broad peak at 11.0 ppm.

2.3 Supramolecular Electrode fabrication

ADMP/KB supramolecular electrodes were fabricated as follows: firstly, the ADMP and KB (1:5) are dissolved in DMF, DMSO or NMP solvents. The slurries were cast onto a carbon paper and is subsequently dried for 12 hours at 60°C in a vacuum oven.

2.4 Characterization of supramolecular electrode

The ^{1}H NMR of the DMSO-d_6 solution was recorded on a A-500 (JEOL). Fourier transform infrared (FT-IR) spectra were measured on a Perkin-Elmer System 2000 by using KBr pellets. UV-vis spectra were recorded on a MultiSpec-1500 (Shimadzu). X-ray photoelectron spectra (XPS) were recorded using a ESCA 850s (Shimadzu). The binding energy was corrected to a peak of 285.0 eV (hydrocarbons).

2.5 Electrochemical measurements

Cyclic voltammogram(CV)s were measured using a BAS electrochemical workstation (100B/W) with a standard three-electrode configuration. A carbon paper (electrode area: 1 cm^2), a Pt wire, and a Ag/AgCl electrode were used as working, counter, and reference electrode, respectively.

3. RESULTS AND DISCUSSION

The criteria of the selecting solvents are the solubility and the stability that are important to give a high rate and high charge utilization to an ADMP/KB nanocomposite. We chose three different aptotic solvents: DMF, DMSO and NMP. Figure 3 shows typical UV-vis spectra of the ADMP in DMF, DMSO and NMP. In NMP the absorption maximum is observed at 366 nm corresponding to the π-π^* transition of pyrimidine moiety of the ADMP. Whereas in the case of DMSO and DMF, a significant (20 nm) red shift is observed for this peak.

The red-shft observed for DMF and DMSO indicated that the structure responsible for supramolecular ribbons are promoted by the solvation of acid-base interaction [24] between the carbonyl group (-R=O) and thiol group (R'-S-H) (Scheme 4).

As scheme 4, it is indicated that nucleotide-like

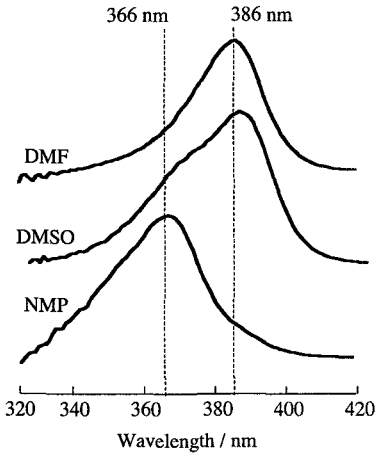

Fig.3 UV-vis spectra for ribbon-formed ADMP supramolecule in various solutions: DMF, DMSO, and NMP.

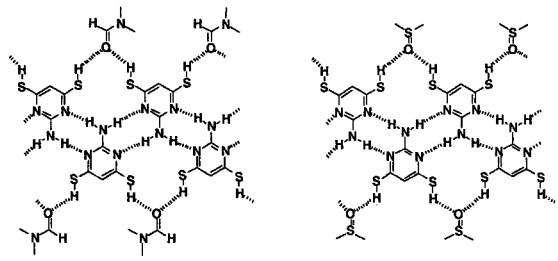

DMF-ADMP DMSO-ADMP

Scheme 4

amino-pyrimidine networks are easily formed with DMF or DMSO assistance via hydrogen bond resulting in a more stable and larger ribbon structures [1, 2, 7]. The difference of promoting ribbon-formed network can be correlated with molecular size or steric hindrance of solvents. The red-shift is a good indication of the formation of molecular aggregation possibly ribbon supramolecules. In fact, similar red-shift effect [8] was found for a disc-shaped supramolecules (benzoylamino-2,2'-bipyridyl-benzene-1,3,5-tricarbonamide derivatives) which associate one another as columnar stacks.

We performed XPS measurement to confirm the interaction between ribbon-form ADMP supramolecules and KB surfaces. Figure 4 shows XPS spectra of N_{1s} for ADMP/KB electrode cast from NMP, DMSO and DMF solutions. N_{1s} spectra indicated that the peaks of aminopyrimidine moiety prepared from DMF (397.1 eV) appears more negative (400.0 ~ 399.1 eV) than that prepared from NMP or DMSO. It is suggested that π interaction increases between aminopyrimidine of ADMP and KB surfaces with increasing association degree of ADMP ribbons.

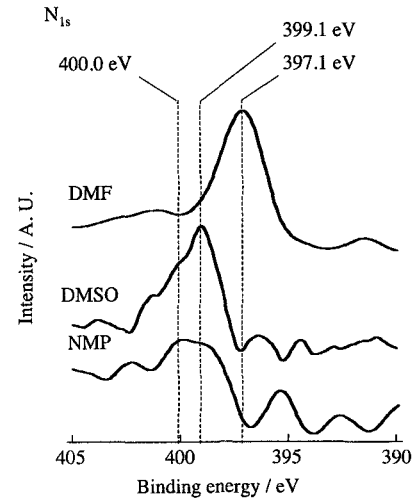

Fig.4 XPS spectra of N_{1s} for ribbon-formed ADMP supramolecule electrode prepared from various cast solutions.

In XPS N_{1s} spectra for aminopyrimidine moiety, there are two kinds of nonequivalent chemical shifts, viz., $-NH_2$ (401.0 eV) and pyrimidine ring (399.4 eV) [25]. The negative shift is also shown in the case of [O-Cu(I)-aminopyrimidine] where the two of N_{1s} spectra appeared at 398.4 and 397.0 eV that are shifted by 2eV due to the π-complex (Cu(I)-pyrimidine) formation [25]. UV-vis and XPS spectroscopies support the evidence of the existence of a long repeating structure of the ribbon-formed ADMP supremolecules in DMF (Figure 5).

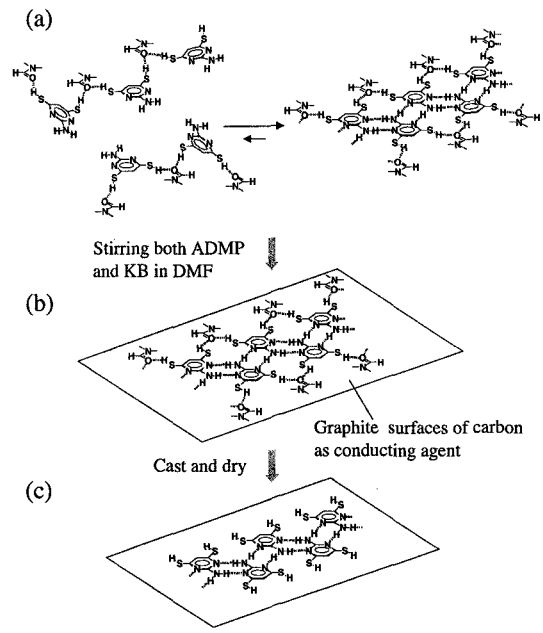

Fig.5 Schematic illustration for the preparations of ribbon-formed ADMP supramolecular/KB electrode.

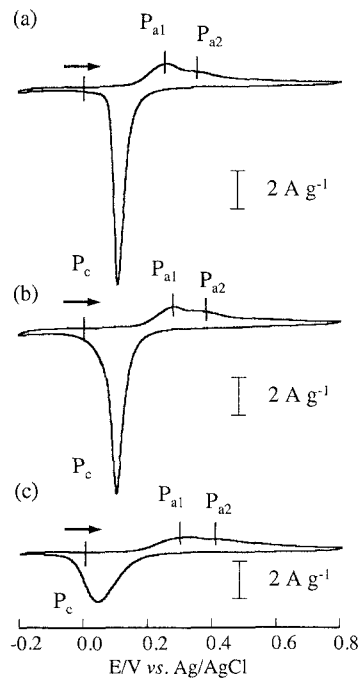

Fig.6 Cyclic voltammograms for the ADMP/acetylene black electrode in 4 M H_2SO_4 aq. Scan rate: 10 mV s^{-1}. Cast solutions: (a) NMP, (b) DMSO, and (c) DMF.

Figure 6 shows cyclic voltammograms for the ADMP/acetylene black electrodes cast from the same three solutions. There are two oxidation peaks and one reduction peak. In oxidization reaction, P_{a1} corresponds to the dimerization of ADMP and P_{a2} corresponds to the oligomerization by the disulfide bond formation. In the reduction reaction, P_c denotes the deoligomerization by the cleavage of disulfide bonds. In DMF solution, the peak separation is narrower and the current value is higher than the others. The redox process can be enhanced by an increase in the association number of ADMPs. It is implied that increasing repetition unites of ADMP supramolecules adsorbed on carbon surface has brought a favored accommodation for the electron and/or proton transfer.

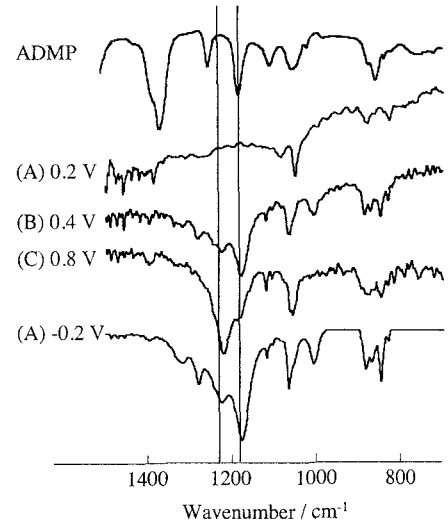

Fig.7 FT-IR spectra for ribbon-formed ADMP supramolecule electrode at different each redox potentials in 4 M H_2SO_4 aq.

Figure 7 shows FT-IR spectra for ADMP bulk material and ADMP electrode cast from DMF. We scanned the potential from 0.2 up to 0.8 and 0.8 down to −0.2 V. Table II shows major FT-IR bands and their possible assignments. The bands at 860-880, 1000-1060, 1180-1200, 1360, and 1400 cm^{-1} are assigned as the C-S stretching, the C-N stretching of primary amine, the C-N stretching of pyrimidine, the N=C-S of thioamide, and the N-C=S of thioamide, respectively [26-28]. At 0.2 V, the peak at 1180 cm^{-1} (pyrimidine ring) disappered. At 0.4V, the peak around 1300-1320 cm^{-1} appeared. This means that the peak of the pyimidine ring (C-N streching) and the sulfuric acid (SO_2 stretching) emphasized when the oxidative dimerization proceeds. At 0.4 V where the dimerization ocurrs (Form B in Figure 8), the peak at 1180 cm^{-1} (the C-N stretching of pyrimidine) appeared. At 0.8 V, the same peak shifted to 1200 cm^{-1}, and the peak around 1400 cm^{-1} (assigned as N-C=S of thioamide) appeared when oxidation further proceeds to form

Table.II FT-IR bands for ribbon-formed ADMP supramolecules electrode each redox potentials and possible assignments.

	Wavenumbers / cm^{-1}				
Possible assignments	ADMP	(A) + 0.2 V	(B) + 0.4 V	(C) + 0.8 V	(A) - 0.2 V
C-S stretching	860	840	860	860	860
		880	880	880	880
C-N stretching of primary amine	1050	1050	1000		1000
	1100	1080	1060	1060	1060
C-N stretching of pyrimidine	1180		1180	1180 (sh)	1180
			1200 (sh)	1200	1200 (sh)
SO_2 stretching of sulfuric acid			1290		1290
			1320	1320	1320
N=C-S of thioamides	1360				
N-C=S of thioamides				1400	1400

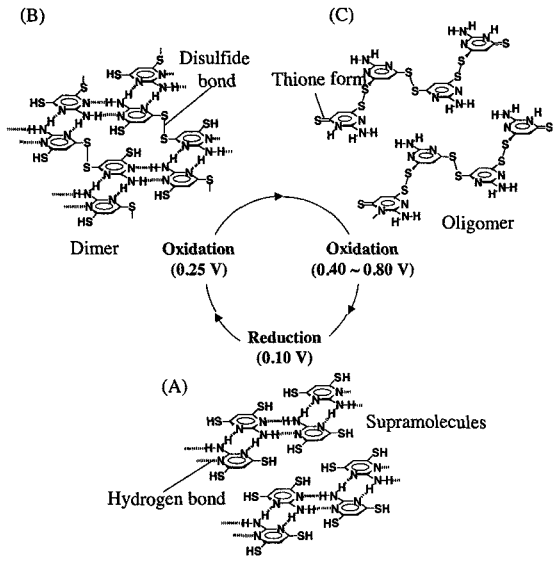

Fig.8 Postulated model of redox reaction scheme for ribbon-formed ADMP supramolecules in proton media.

oligomers. During the negative potential scan, at –0.2 V, the peak of C-N stretching appeared again around 1180 cm^{-1} upon cleavage of disulfide bond (reduction reaction).

In the oxidation process, the positive shift of the peak of the C-N stretching from 1180 to 1200 cm^{-1} is attributed to a decreasing number of hydrogen bonds via aminopyrimidine [29]. At the most oxidized state of 0.8 V, the peak at 1400 cm^{-1} appeared, indicating that the thione structure (C=S) is dominant for ADMP oligomers (Form C in Figure 8). In the reduction process at –0.2V, the peak at 1200 cm^{-1} (the C-N stretching) negatively shifted to 1180 cm^{-1}. It is considered that the ADMP oligomers are reduced to form monomers with supramolecular structures indicated as Form A in Figure 8.

Figure 9 shows a typical cyclic voltammogram for the ADMP/KB nanocomposite electrode. A narrower peak separation (40 mV) is confirmed compared to that in Figure 6(a). This indicates that the ADMP is well fixed on the electrode surface leading to a fast trasformation between thiole and disulfide forms of the ADMP supramolecules (surface wave CV behavior). The interaction between ADMP and KB would be strong because the ADMPs have good adhesion onto KB having following features: a high specific surface area (1270 $m^2\ g^{-1}$), graphite-like surface structure, high porosity (78 %), composed of nanometer ordered primary particles (34 nm) with hollow [30].

Figure 10 shows the scan-rate dependency of the ADMP/KB electrode. The electrode delivered a

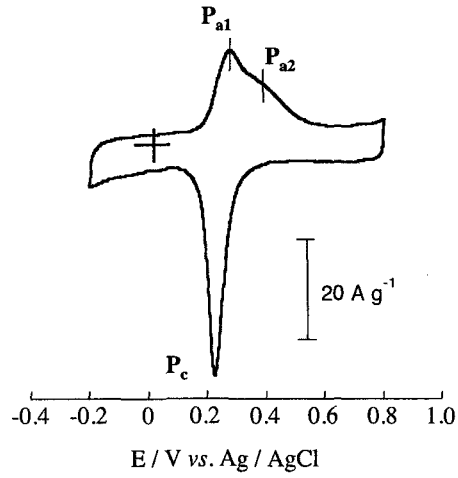

Fig.9 Cyclic voltammogram for ribbon-formed ADMP/KB nanocomposite electrode in 4 M H_2SO_4. Scan rate: 5 mV s^{-1}.

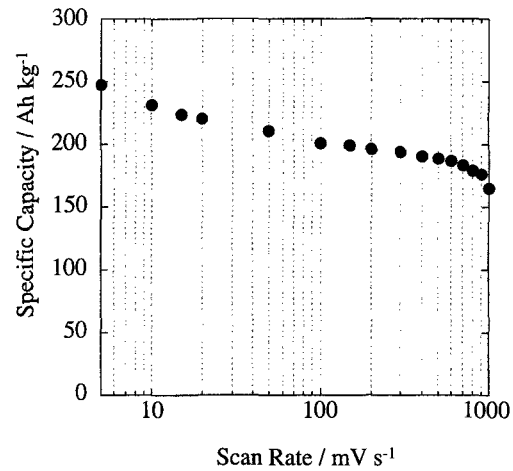

Fig.10 Scan rate dependency of ribbon-formed ADMP/KB nanocomposite electrode in H_2SO_4.

high specific capacity (247 mAh g^{-1}) with high charge utilization (74 %) at 5 mV s^{-1}. Moreover, the composite electrode maintained its high specific capacity of 165 mAh g^{-1} at higher scan rate of 1000 mV s^{-1}.

4. CONCLUSIONS

A novel material of organosulfur ribbon-formed ADMP supramoelcule has been proposed as an energy storage electrode material. We attempted to design a composite made of ADMP and KB. The ADMP/KB nanocomposite electrode delivered high specific capacity (247 mAh g^{-1}) with high charge utilization (74 %) at 5 mV s^{-1}. A high specific capacity of 165 mAh g^{-1} has been maintained at high scan rate of 1000 mV s^{-1}. The improvement in charge utilization and rate capability of the ADMP/KB composite electrode

is considered to be due to the construction of optimized electronic and ionic transfer paths formed between the ribbon-formed ADMP supramolecules and the graphitized surface of KB.

ACKNOWLEDGMENT

The work reported here is a part of the 21st Century COE (Center of Excellence) program of "Future Nano-Materials" research and education project, which is financially supported by Ministry of Education, Science, Sports, Culture, and Technology thorough Tokyo University of Agriculture and Technology.

K.N. and N.O. would like to thank Mr. Y. Igarashi and Ms. Y. Shintaku for their experimental support and useful discussions.

REFERENCES

[1] G. M. Whitesides, J. P. Mathias, and C. T. Seto, *Science*, **vol. 2**, 1312-1319 (1991).

[2] J-M. Lehn, M. Mascal, A. DeCian and J. Fischer, *J. Chem. Soc. Perkin Trans. 2*, 461-467 (1992).

[3] C. T. Seto, and G. M. Whitesides, *J. Am. Chem. Soc.*, **115**, 905-916 (1993).

[4] C. T. Seto, and G. M. Whitesides, *J. Am. Chem. Soc.*, **115**, 905-916 (1993).

[5] C. T. Seto, J. P. Mathias, and G. M. Whitesides, *J. Am. Chem. Soc.*, **115**, 1321-1329 (1993).

[6] C. T. Seto, and G. M. Whitesides, *J. Am. Chem. Soc.*, **115**, 1330-1340 (1993).

[7] A. R. A. Palmans, J. A. J. M. Vekemans, E. E. Havinga, and E. W. Meijer, *Angew. Chem. Int. Ed. Engl.*, **36, No. 23**, 2648-2651 (1997).

[8] L. Brunsveld, H. Zhang, M. Glasbeek, J. A. J. M. Vekemans, and E. W. Meijer, *J. Am. Chem. Soc.*, **122**, 6175-1682 (2000).

[9] S.J. Visco, C.C. Mailhe, L.C. De Jonghe and M.B. Armand, *J. Electrochem. Soc.*, **136**, 661-664 (1989).

[10] M. Liu, S.J. Visco and L.C. De Jonghe, *J. Electrochem. Soc.*, **136**, 2570-2575 (1989).

[11] M. Liu, S.J. Visco and L.C. De Jonghe, *J. Electrochem. Soc.*, **137**, 750-759 (1990).

[12] S.J. Visco, M. Liu, and L.C. De Jonghe, *J. Electrochem. Soc.*, **137**, 1191-1192 (1990).

[13] M. Liu, S.J. Visco and L.C. De Jonghe, *J. Electrochem. Soc.*, **138**, 1891-1895 (1991).

[14] M. Liu, S.J. Visco and L.C. De Jonghe, *J. Electrochem. Soc.*, **138**, 1896-1901 (1991).

[15] M.M. Doeff, S.J. Visco and L.C. De Jonghe, *J. Electrochem. Soc.*, **139**, 1808-1812 (1992).

[16] M.M. Doeff, M.M. Lerner, S.J. Visco and L.C. De Jonghe, *J. Electrochem. Soc.*, **139**, 2077-2081 (1992).

[17] T. Sotomura, H. Uemachi, K. Takeyama, K. Naoi, and N. Oyama, *Electrochim. Acta.*, **37**, 1851-1854 (1992).

[18] K. Naoi, Y. Iwamizu, M. Mori, and Y. Naruoka, *J. Electrochem. Soc.*, **144,** 1185-1188 (1997).

[19] K. Naoi, K. Kawase, M. Mori, and M. Komiyama, *J. Electrochem. Soc.*, **144,** L173-L175 (1997).

[20] S. Picart, and E. Genies, *J. Electroanal. Chem.*, **408,** 53-60 (1996).

[21] K. Naoi, S. Suematsu, M. Komiyama, and N. Ogihara, *Electrochim. Acta.*, **47**, 1091-1096 (2002).

[22] J. W. Steed and J. L. Atwood, "Supramolecular Chemistry", John Wiley & Sons, Ltd (2000) pp. 22-24.

[23] S. Ooae, "Organ sulfur chemistry", Kagakudouzin, (1982).

[24] T. J. Wallace, *J. Am. Chem. Soc.,* **86,** 2018-2021 (1964).

[25] Q. Miao, X. Yie, X. Xin, H. Adachi, and I. Tanaka, *Applied Surface Science,* **171,** 49-56 (2001).

[26] D. Lin-Vien, N. B. Colthup, W. G. Fateley, and J. G. Grasselli, "The Handbook of Infrared and Raman Characteristic Frequencies of Organic Molecules", Academic Press Inc., (1991).

[27] F. R. Dollish, W. G. Fateley, and F. F. Bently, "Characteristic Raman Frequencies of Organic Compounds," Wily, New York (1974).

[28] S. K. Freeman, "Applications of Laser Raman Spectroscopy," Wiley Interscience, New York (1974).

[29] K. Naoi, A. Shimada, S. Suematsu, and K. Machida, *Electrochemistry,* **69,** 447-450 (2001).

[30] "Catalog of Ketjen Black", Ketjen Black International Company, (2001) pp.5

(Received October 13, 2003; Accepted March 16, 2004)